Spintronics -1

Outline

- Spin Transfer Torque
- Pure Spin current (no net charge current)
  - Spin Hall, Inverse Spin Hall effects
  - Spin Pumping effect
  - Spin Seebeck effect
- Micro and nano Magnetics

Spin Transfer Torque

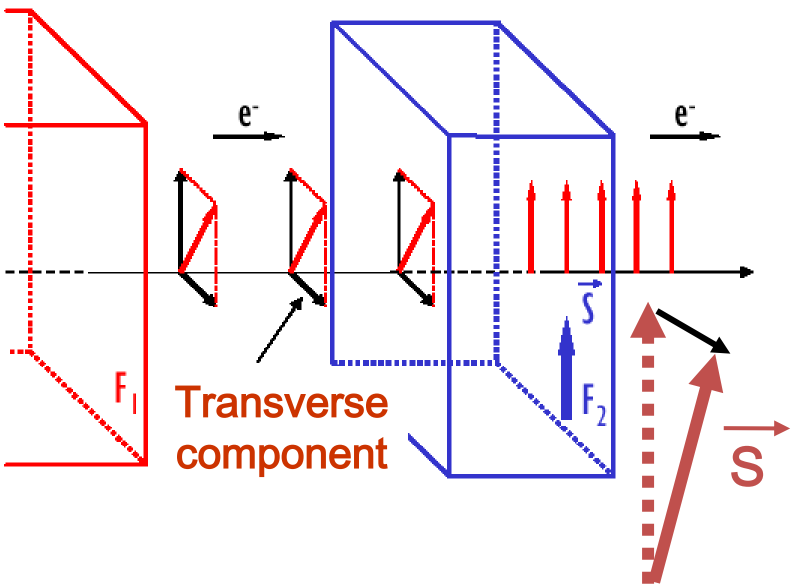

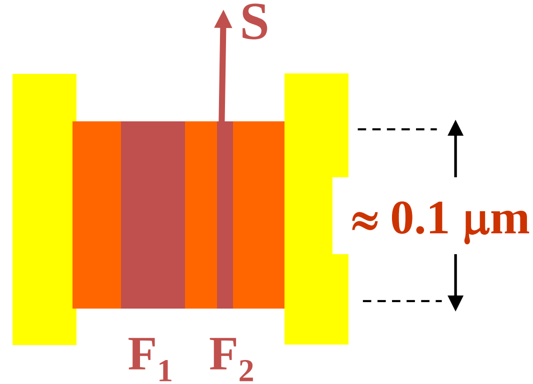

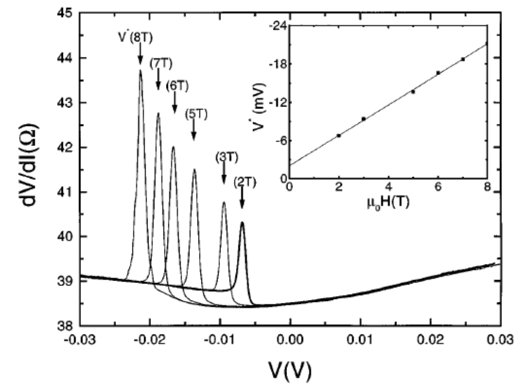

FIG. 1. The point contact $dV/dI(V)$ spectra for a series of magnetic fields (2, 3, 5, 6, 7, and 8 T) revealing an upward step and a corresponding peak in dV/dI at a certain negative bias voltage $V^*(H)$. The inset shows that $V^*(H)$ increases linearly with the applied magnetic field H.

Tsoi et al. PRL **61**, 2472 (1998)

The transverse spin component is lost by the conduction electrons, transferred to the global spin of the layer $\vec{S}$

$$\dot{S}_{1,2} = (I_e g/e)\,\hat{s}_{1,2}\times(\hat{s}_1\times\hat{s}_2)$$

Slonczewski JMMM **159**, L1 (1996)

Modified Landau-Lifshitz-Gilbert (LLG) equation

$$\frac{dm}{dt} = -\gamma m\times H_{eff} + \alpha m\times\frac{dm}{dt} + \frac{\gamma\hbar PI}{2e\mu_0 M_S V}(m\times\sigma\times m)$$

Experimantally determined current density ~10^{10}-10^{12}A/m^2

Spin Transfer Torque

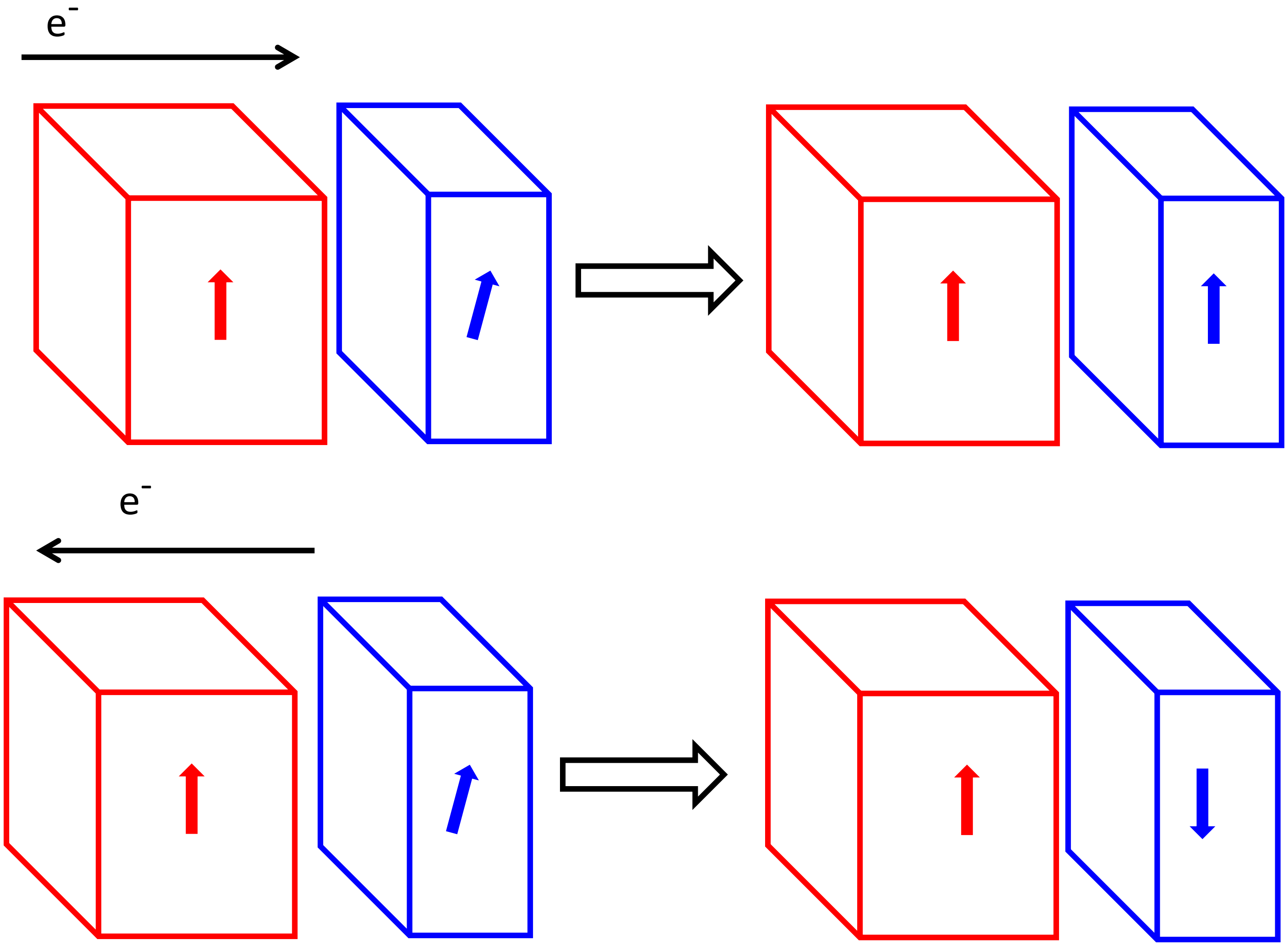

In a trilayer, current direction determines the relative orientation of F1 and F2

Spin Transfer Torque

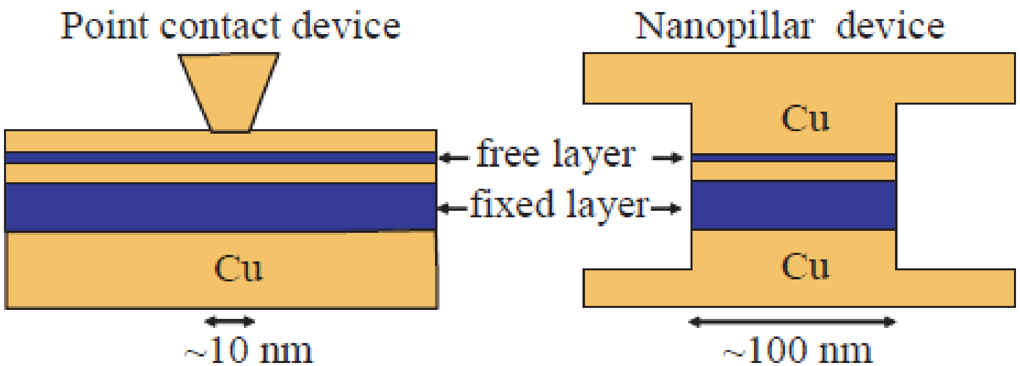

Ralph and Stiles:
"Spin transfer torques". *JMMM* **320,** 1190–1216 (2008).

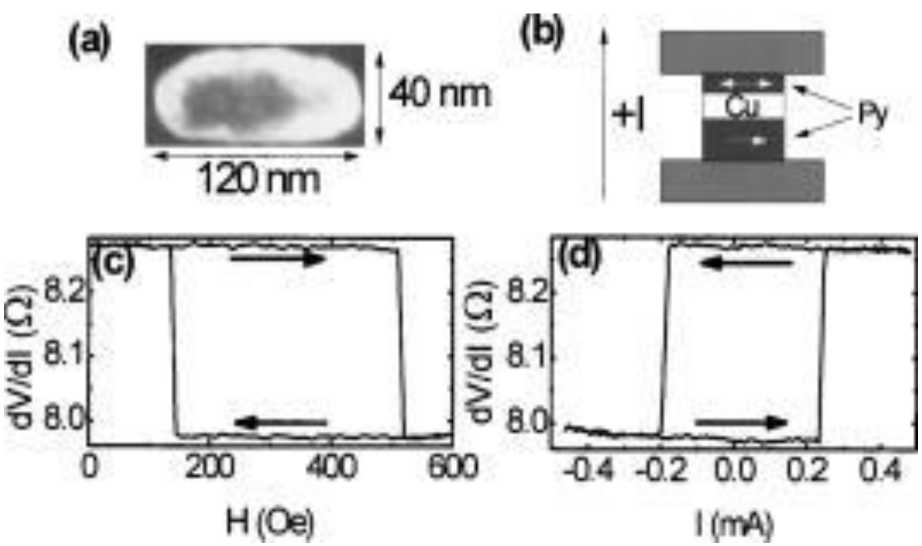

(c) Minor loop of free layer and
(d) spin transfer curve at 293*K*
120 Cu/20 Py/12 Cu/X Py/2 Cu/30 Au

Ralph and Buhrman's group, APL **87**, 112507 (2005)

Spin Transfer Torque

Landau-Lifshitz-Gilbert equation with Spin Transfer Torque terms

Current induced domain wall motion

Passing spin polarized current from Domain A to Domain B⇒B switches

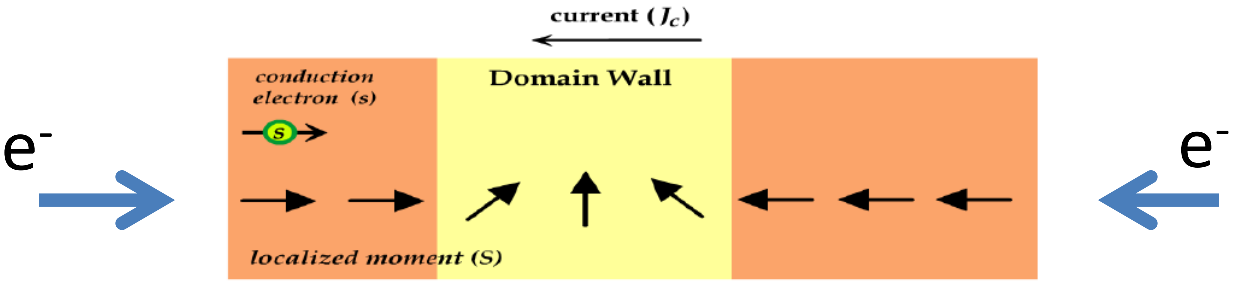

Domain A Domain B

$$\frac{\partial \vec{M}}{\partial t} = -\gamma \vec{M} \times \vec{H}_{eff} + \frac{\alpha}{M_s} \vec{M} \times \frac{\partial \vec{M}}{\partial t} + \vec{T}_{STT}$$

Berger, *JAP* **55**, 1954 (1984)
Tatara *et. al.*, *PRL* **92**, 086601 (2004)
Zhang *et. al.*, *PRL* **93**, 127204 (2004)
Thiaville *et. al.*, *Europhys. Lett*. **69**, 990 (2005)
Stiles *et. al.*, *PRB* **75**, 214423 (2007)

Spin Transfer Torque

Landau-Lifshitz-Gilbert equation with Spin Transfer Torque terms

$$\frac{\partial \vec{M}}{\partial t} = -\gamma \vec{M} \times \vec{H}_{\text{eff}} + \frac{\alpha}{M_s} \vec{M} \times \frac{\partial \vec{M}}{\partial t} - \frac{b_j}{M_s^2} \vec{M} \times \left(\vec{M} \times \frac{\partial \vec{M}}{\partial x}\right) - \frac{c_j}{M_s} \vec{M} \times \frac{\partial \vec{M}}{\partial x} \qquad b_j, c_j \sim JP/t$$

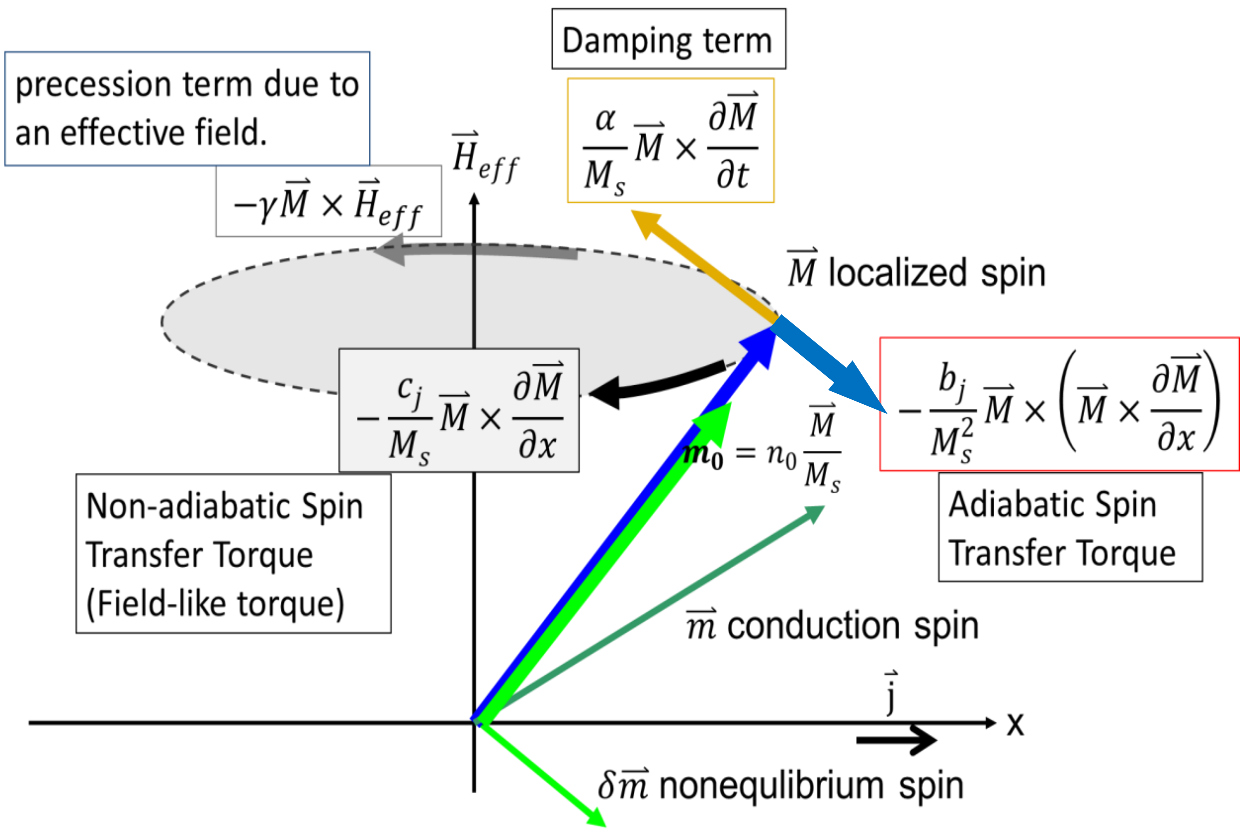

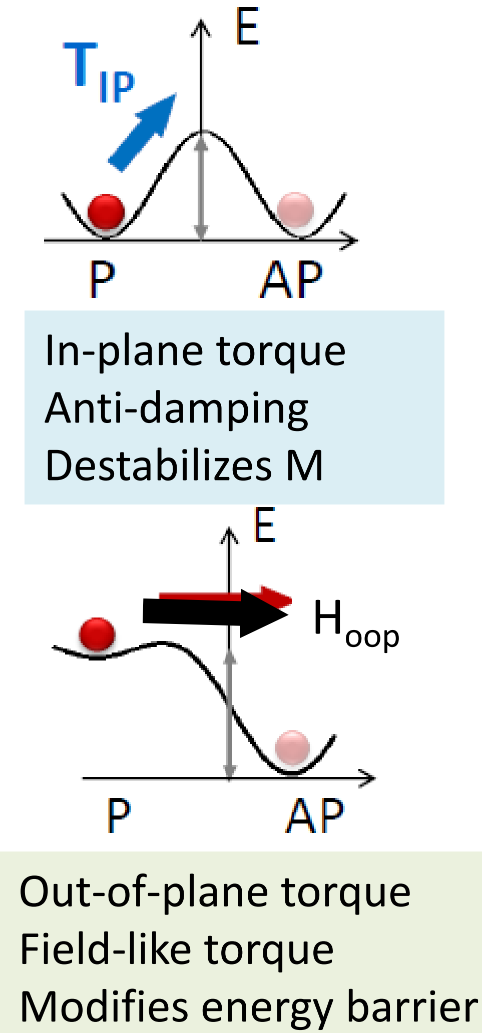

Onsager reciprocity relations

Conjugate variables

X_i generalized forces

J_i generalized currents

$J_i = \sum_j L_{ij} X_j$ linear response

$i = \{\text{mass, charge, spin, energy, …}\}$

$\dot{S} = \sum_i X_i J_i$ entropy creation rate

$$L_{ij}(\mathbf{m}, \mathbf{H}_{ext}) = \varepsilon_i \varepsilon_j L_{ji}(-\mathbf{m}, -\mathbf{H}_{ext})$$

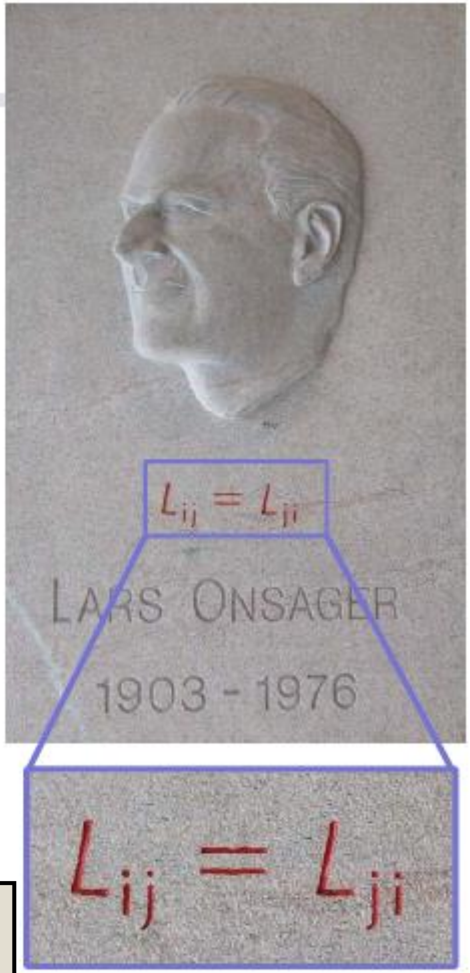

Equality between certain relations between flows and forces out of equilibrium

Currents can induce magnetization excitations

↕

A time-dependent magnetization can induce (charge and spin) currents

Industrial applications

Read head in hard drives

MRAM

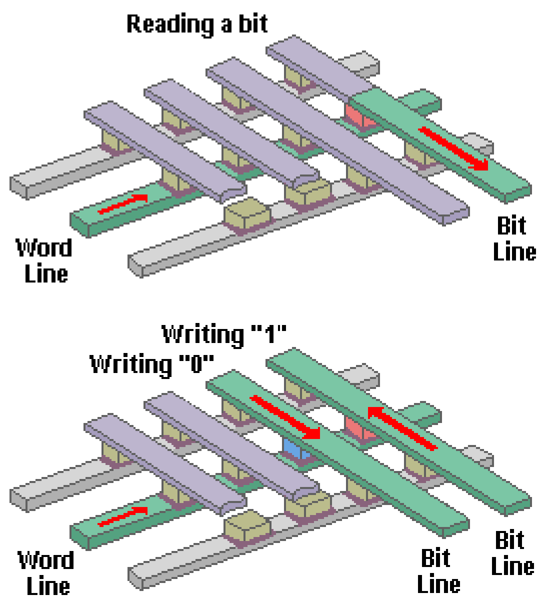

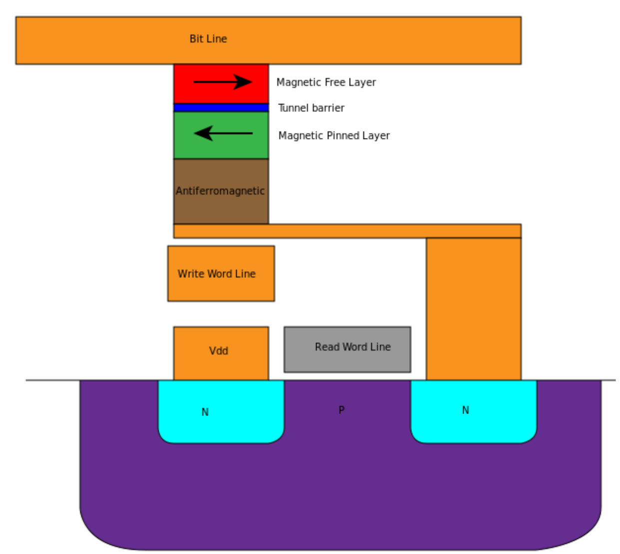

Application of Spin Transfer Torque

Magnetic Domain-Wall Racetrack Memory

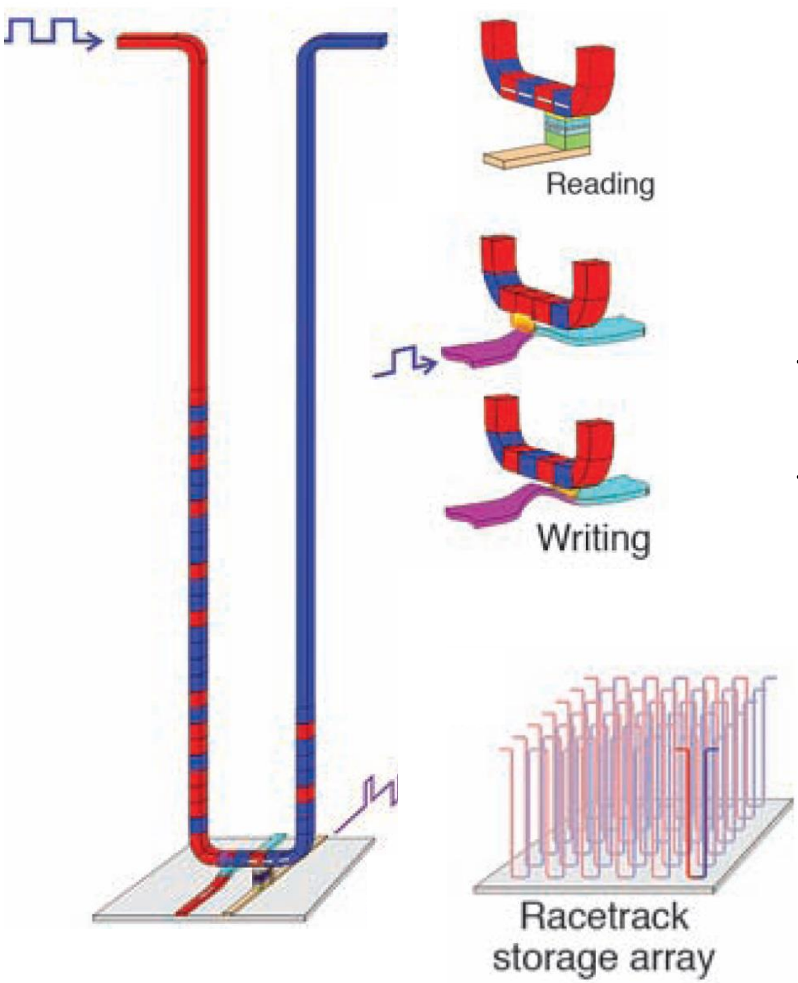

Dr. Stuart S. P. Parkin Science **320**, 190 (2008)

A novel three-dimensional spintronic storage class memory

Magnetic nanowires: information stored in the domain walls

- Immense storage capacity of a hard disk drive

- High reliability and performance of solid state memory (DRAM, FLASH, SRAM...)

→ **Understanding of current induced domain wall (DW) motion**

Application of Spin Transfer Torque

Domain Wall Structures in Permalloy Nanowires

(a)

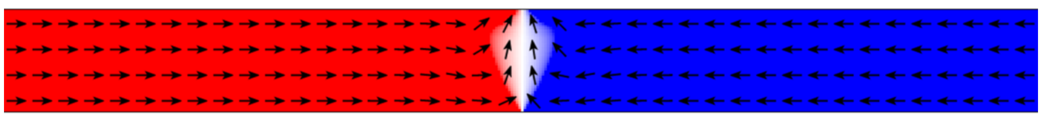

Transvers DW

(b)

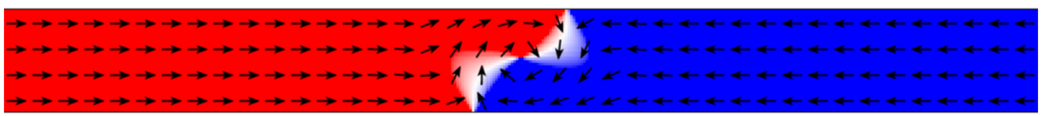

Vortex DW

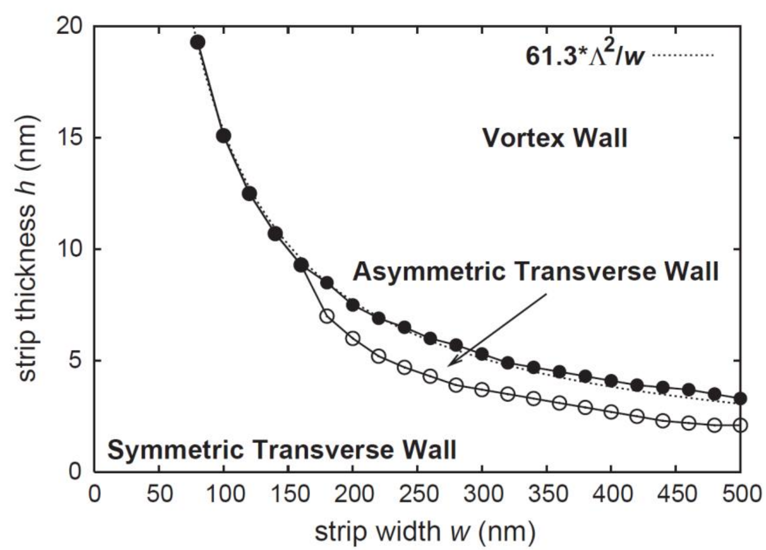

J. Magn. Magn. Mater. **290**, 750 (2005)

DW traps

protrusion

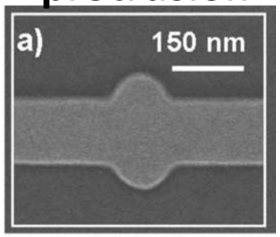

notch

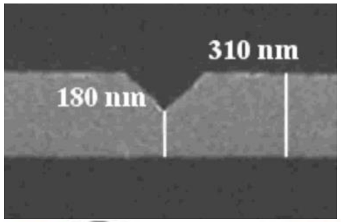

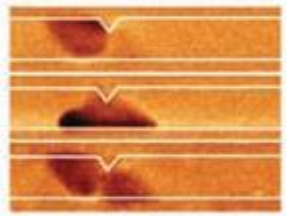

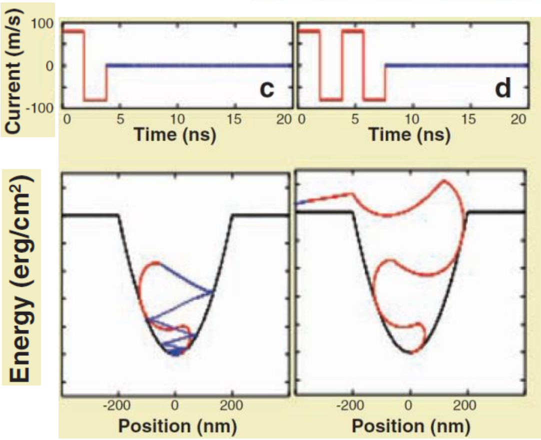

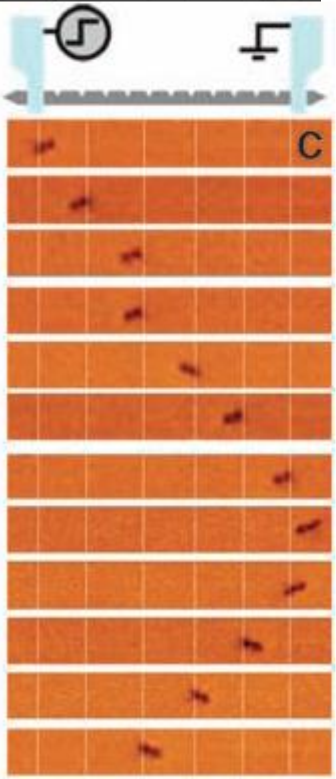

Application of Spin Transfer Torque

DW Oscillators

$j_W < j_a < j_{dep}$

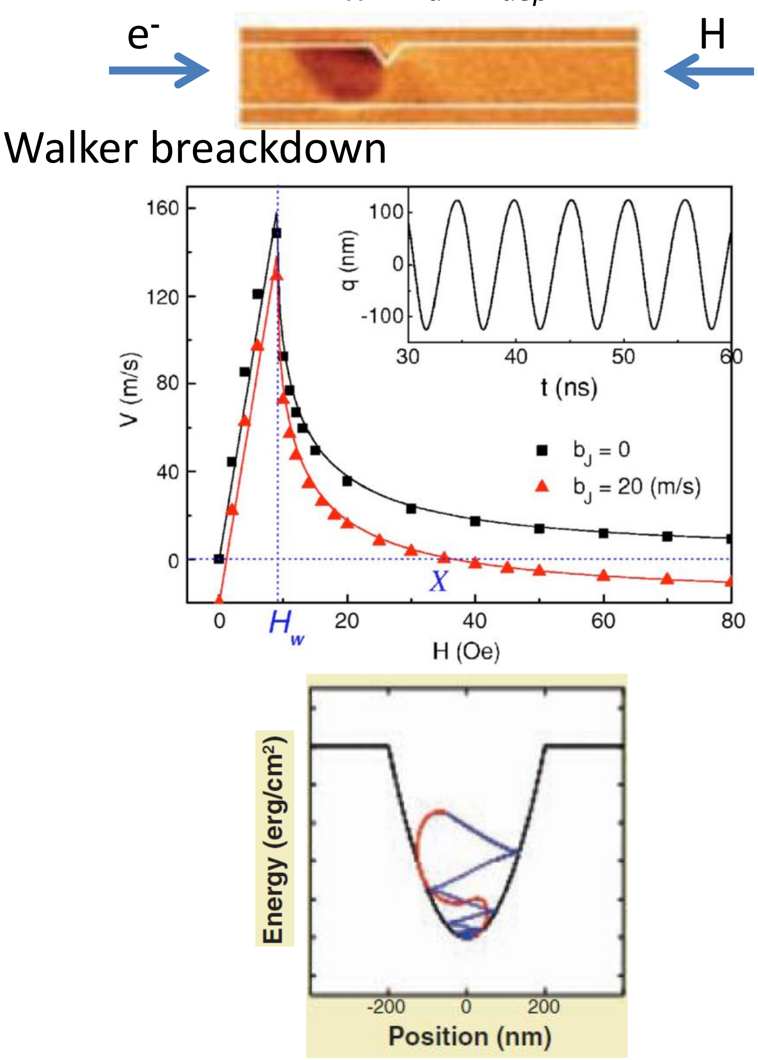

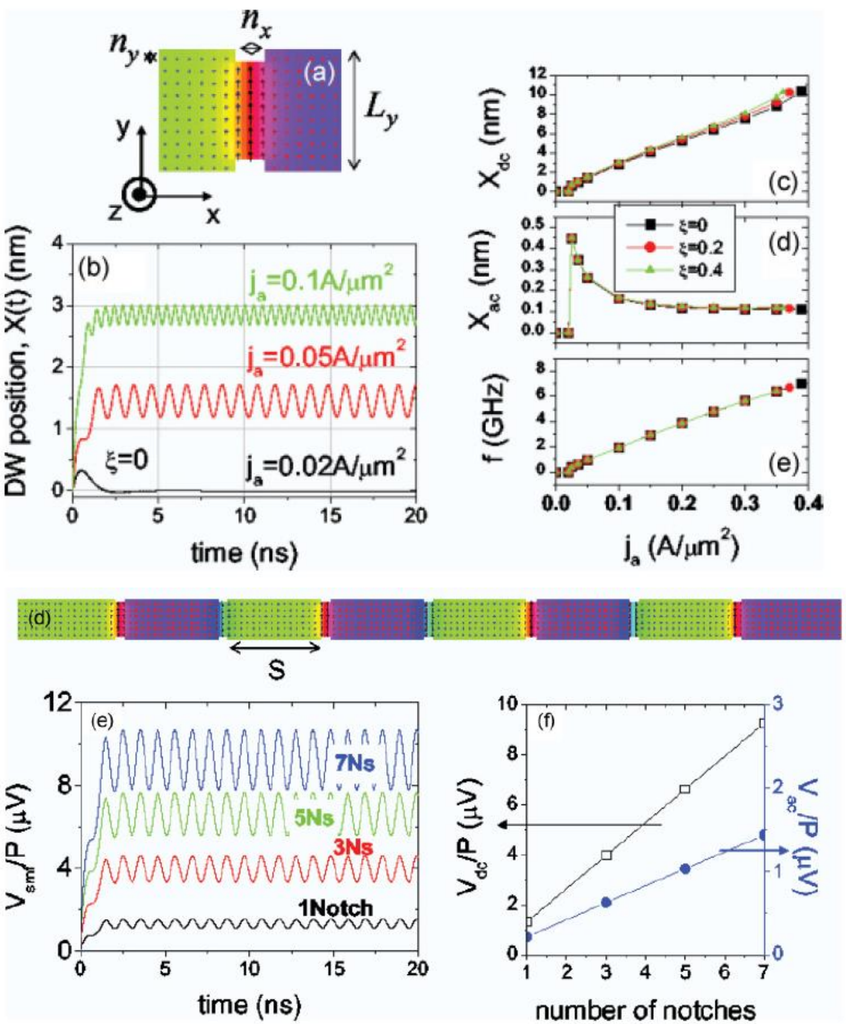

Phys. Rev. B **83**, 174444 (2011)
Appl. Phys. Lett. **90**, 142508 (2007)

Application of Spin Transfer Torque

AC Current-Induced DW Resonance

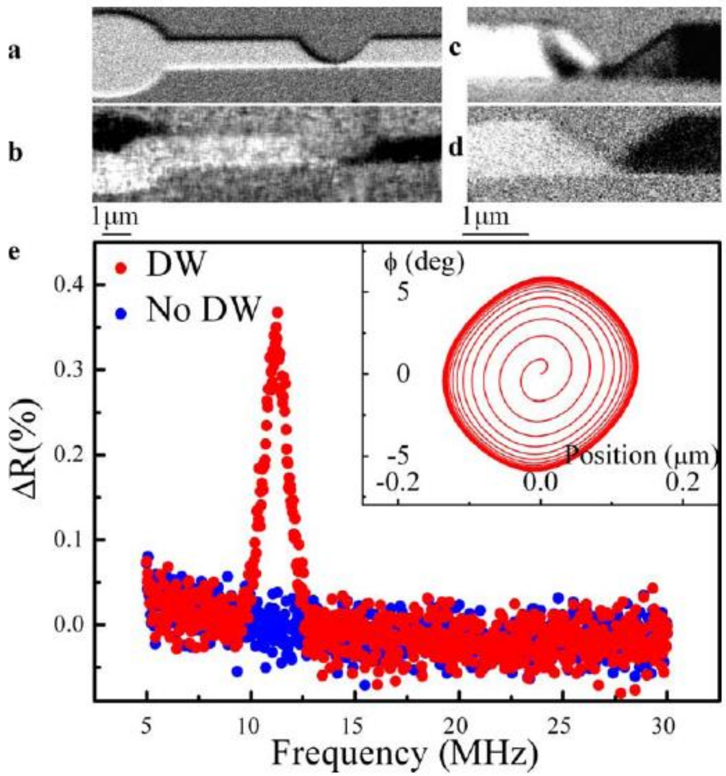

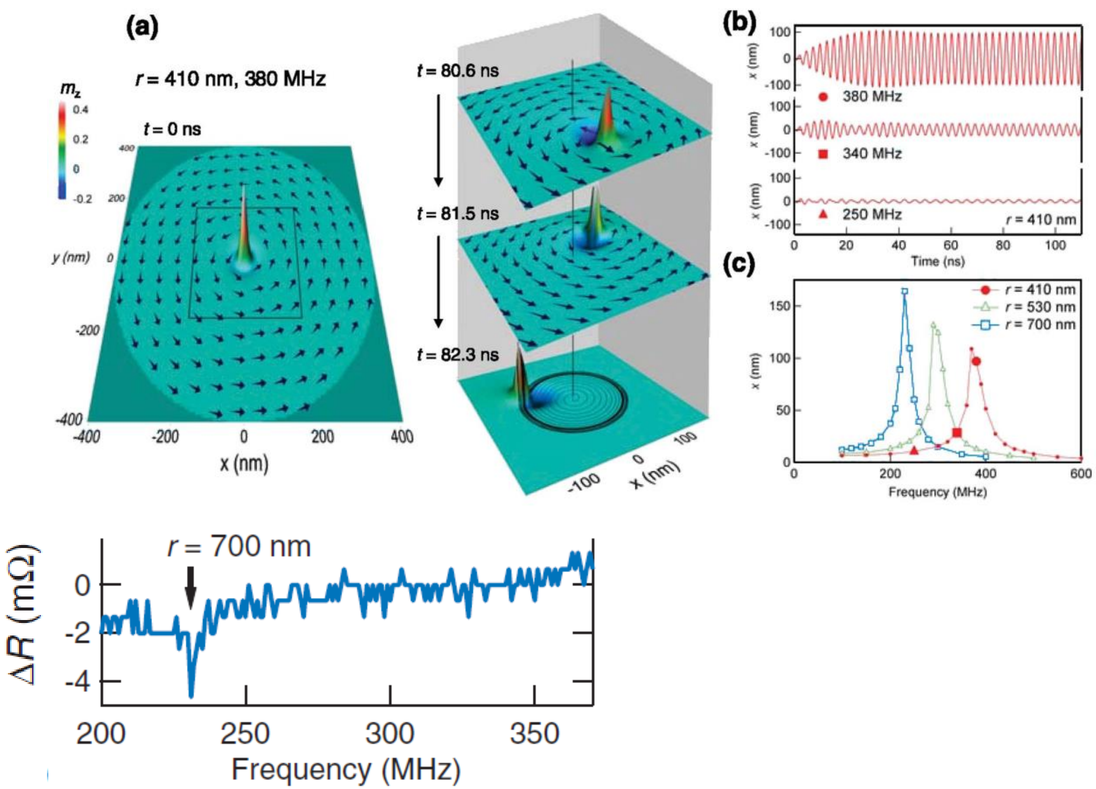

PRB **81**, 060402 (2010), PRL **97**, 107204 (2006)

Application of Spin Transfer Torque

Radio-Frequency DW Oscillators

AC

DC

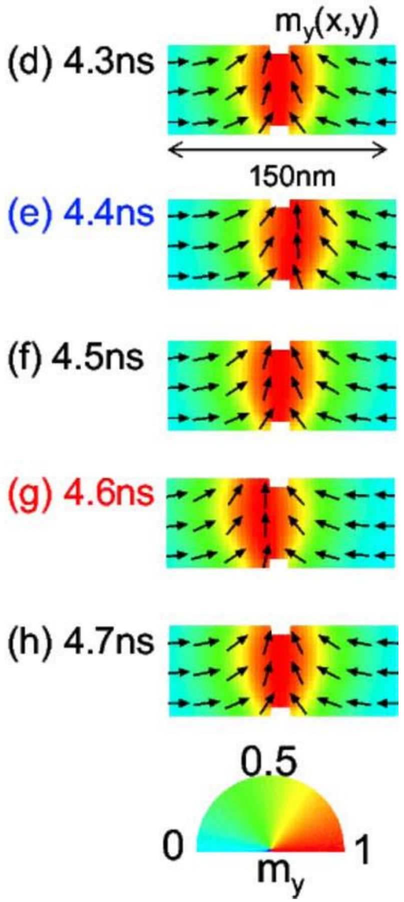

CPP-nanopillar

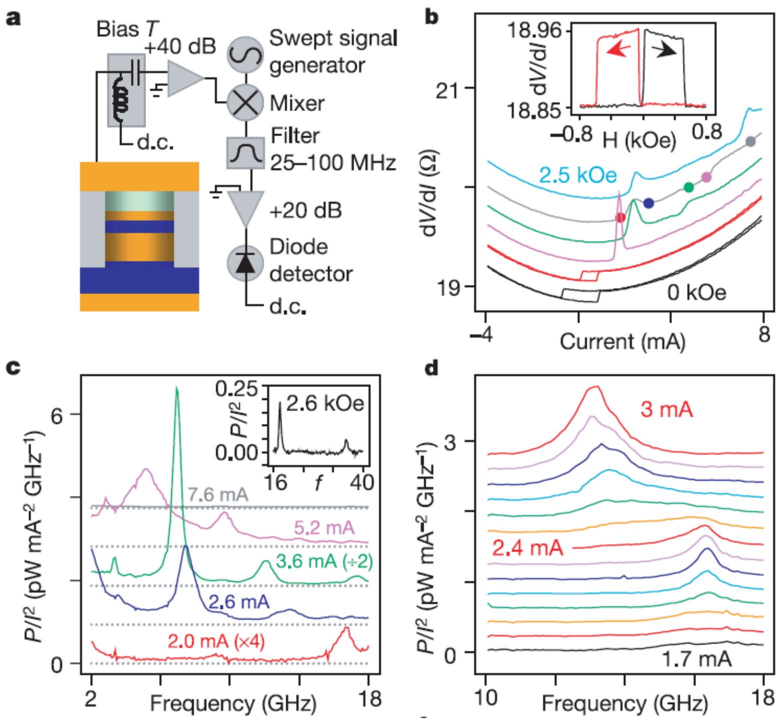

Nature **425**, 380 (2003)

Outline

- Spin Transfer Torque
- Pure Spin current (no net charge current)
    - Spin Hall, Inverse Spin Hall effects
    - Spin Pumping effect
    - Spin Seebeck effect
- Micro and nano Magnetics

Nano Magnetism

Vortex induced by dc current in a circular magnetic spin valve nanopillar

L. J. Chang and S. F. Lee

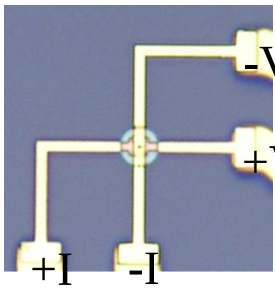

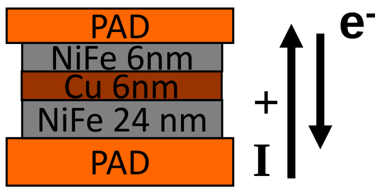

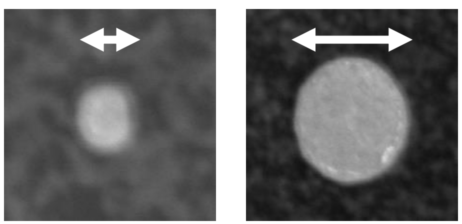

90 nm 380 nm

oommf

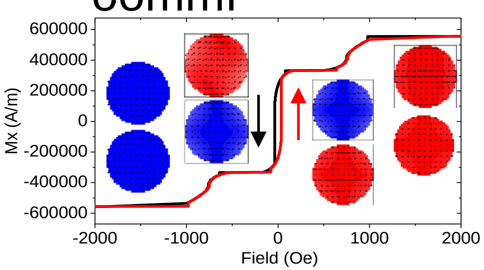

D = 90 nm

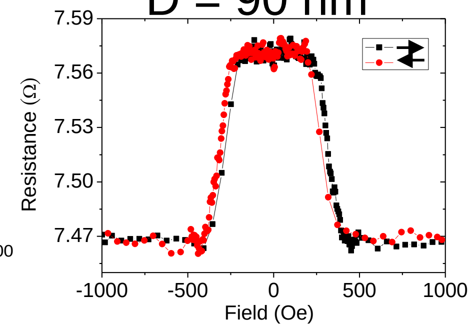

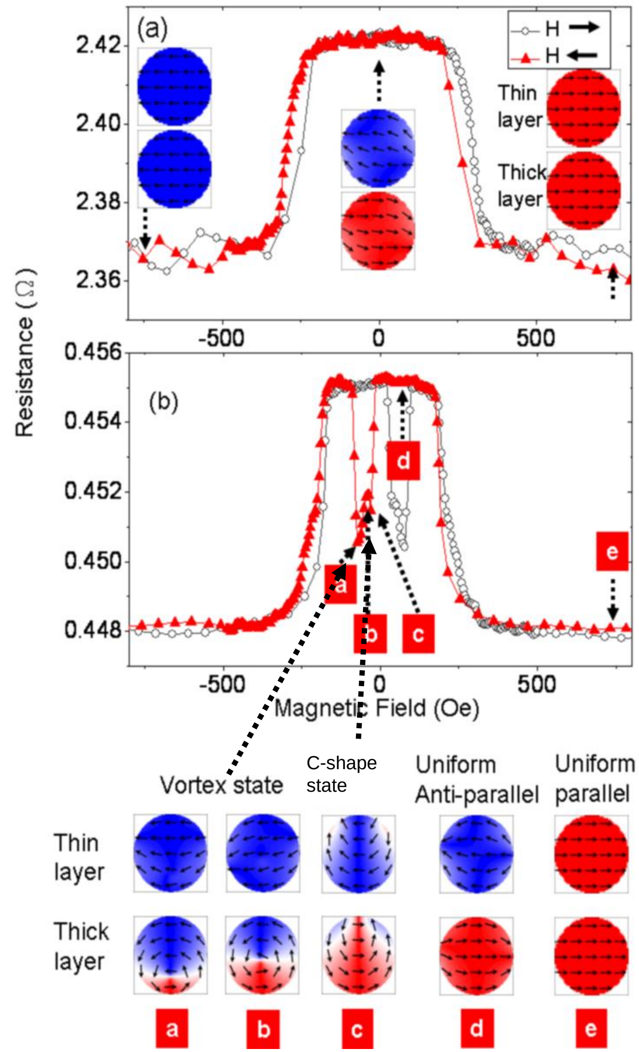

D = 160 nm

D = 380 nm

Current driven vortex nucleation

D = 160 nm H = 0 Oe

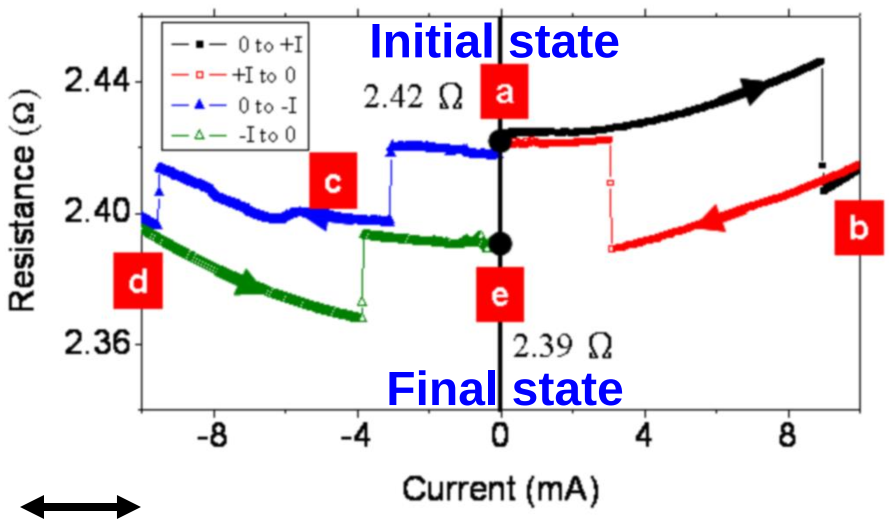

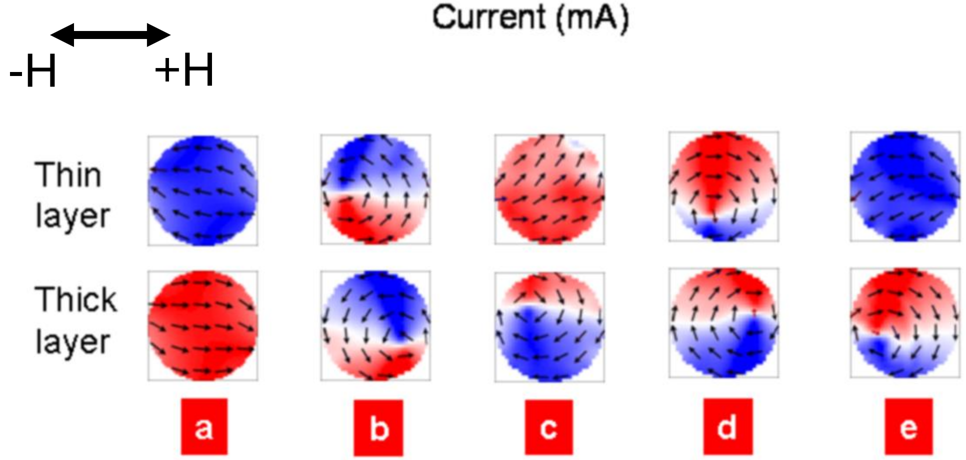

Other research interest include superconductor-magnetic material proximity effect, Ferromagnetic Resonance etc.

Domain wall oscillation in a trapping potential

Theoretical Backgrounds

Resonant DW induced by AC spin-polarized current in Ferromagnetic strips

DW dynamics equation

$$(1+\alpha^2)m\frac{d^2x}{dt^2} = F_p(x) + F_f + F_s + F_d$$

where $m = \frac{2(\mu_0 L_y L_z)}{\gamma_0^2 (N_z - N_y)\Delta_0}$ is the effective DW mass (kg), and the other variables are listed below.

L_y : width of wire (m)

L_z : thickness of wire (m)

μ_0 : permeability ($4\pi \times 10^{-7}$ $VsA^{-1}m^{-1}$)

γ_0 : electron gyromagnetic ratio (2.2×10^5 $Vs^2m^{-1}kg^{-1}$)

N_z, N_y : transverse demagnetizing factors

Δ_0 : DW width (m)

x : DW position (m)

Experiment Methods

four point probe measurement circuit

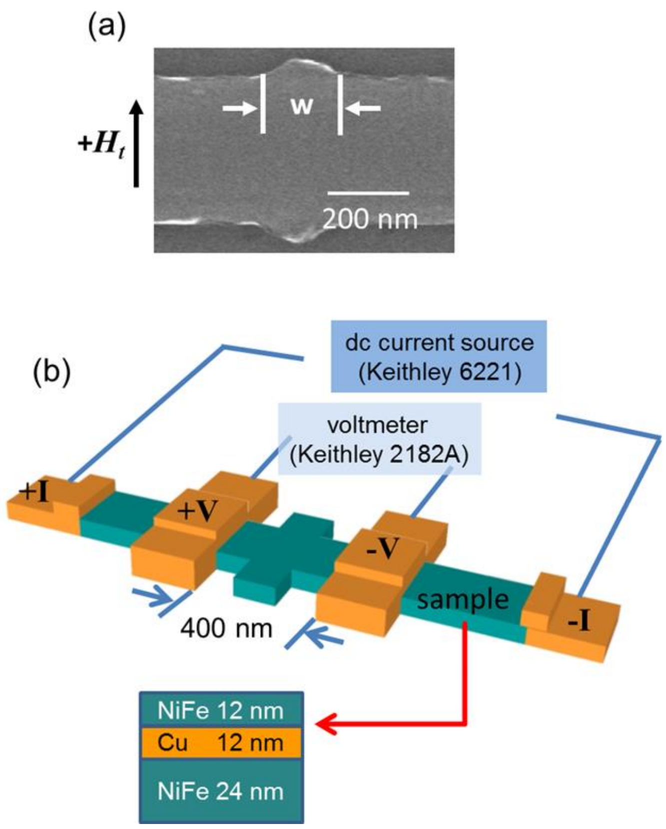

high frequency measurements circuit

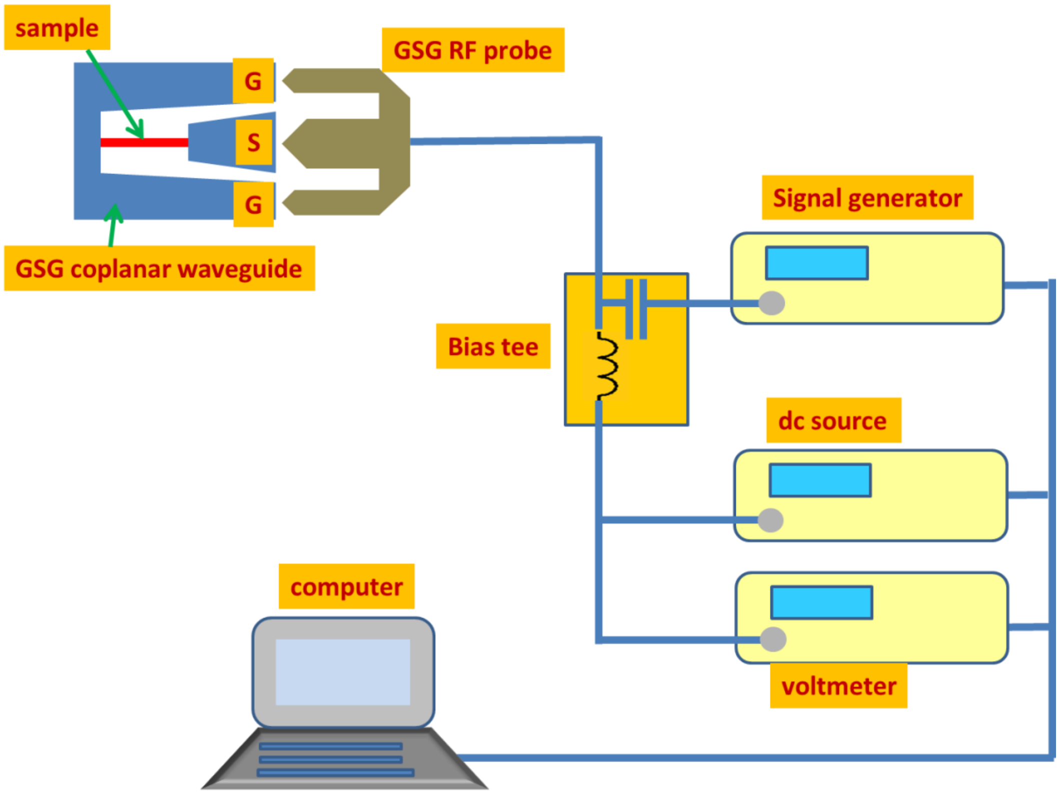

Measurement and simulation results

AC current induced localized domain wall oscillators in NiFe/Cu/NiFe submicron wires

Nucleation of Pinned anti-parallel transverse DW

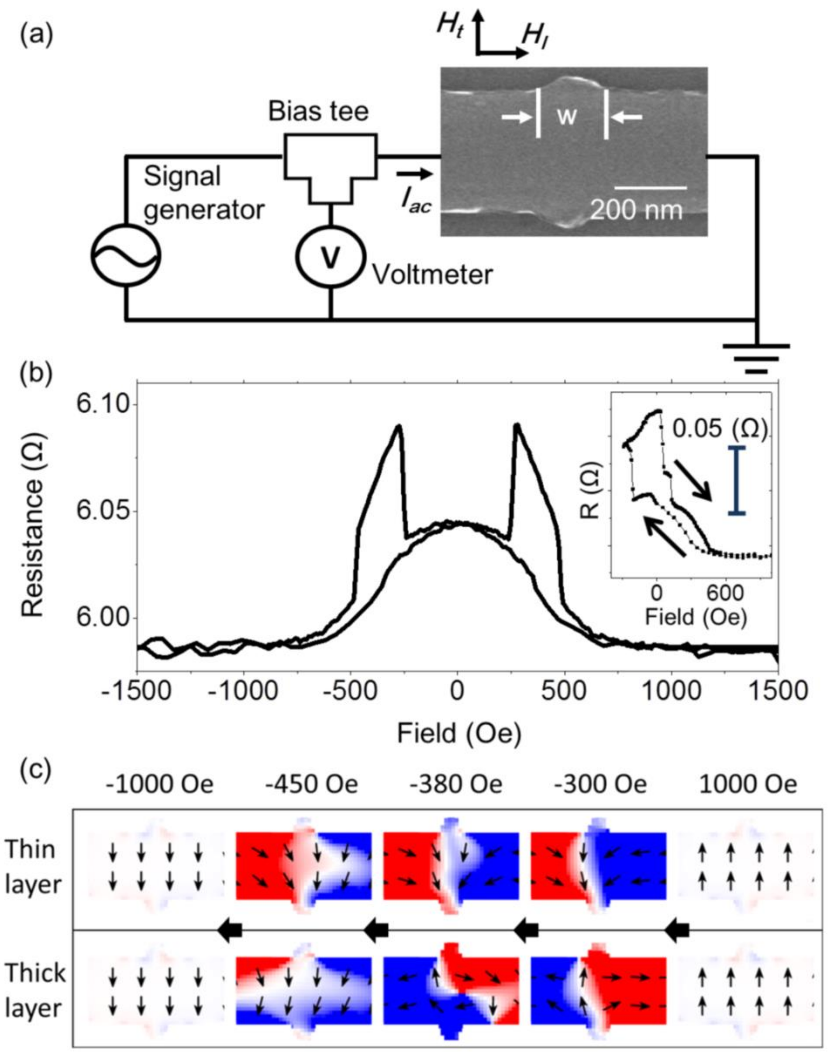

Measurement and simulation results

AC current induced localized domain wall oscillators in NiFe/Cu/NiFe submicron wires

DW resonators for frequency-selective operation

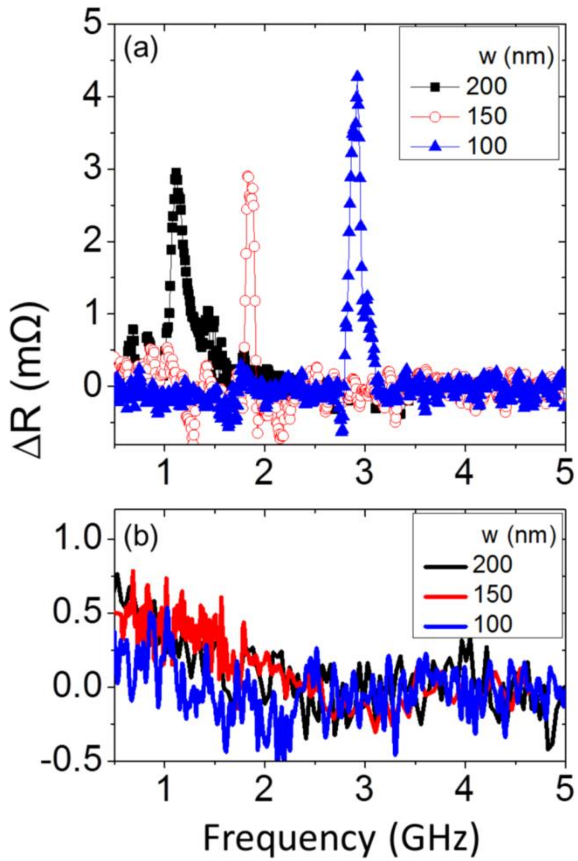

(a) Experimental measurement of the ac current induces resonance excitation of pinned DW trapped at the protrusion. Resistance change as a function of ac excitation current frequency for the submicron wires containing artificial symmetric protrusions with three different widths of protrusion w = 200, 150, and 100 nm. (b) The response curve measured at the saturation field with a uniform state of submicron wires (without DW). The ΔR is observed unchanged with frequency for each of the samples.

Measurement and simulation results

AC current induced localized domain wall oscillators in NiFe/Cu/NiFe submicron wires

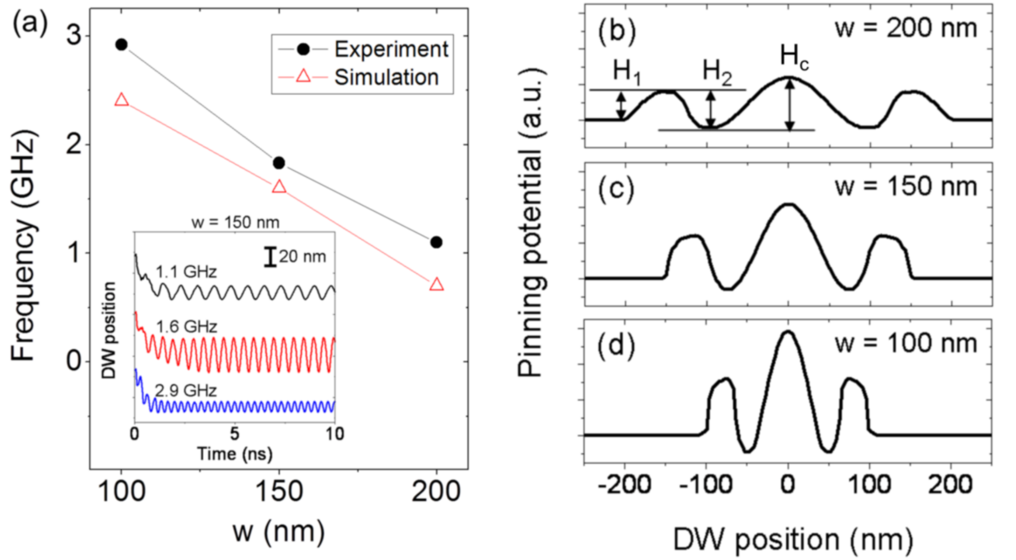

Resonance frequency of pinned DW dependence on the width of trap w, the solid circles and the open triangles indicate the experiment and simulation results respectively. The inset shows the simulated time evolutions of the DW motion with w = 150 nm. (b)-(d) Potential landscape of pinned DW from micromagnetic simulation with three different width of protrusion w = 200, 150, 100 nm.

Measurement and simulation results

Reversible domain wall motion induced by dc current in NiFe/Cu/NiFe submicron wires

nano-pillar

Current in-plane

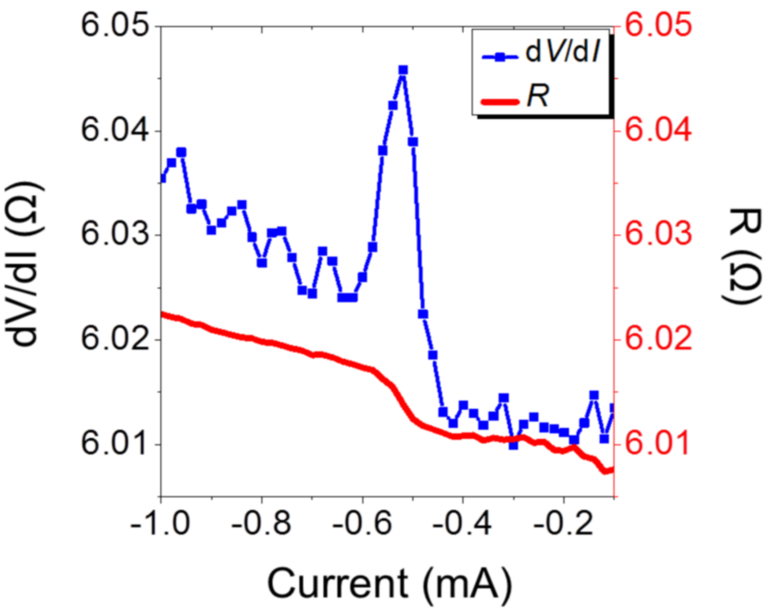

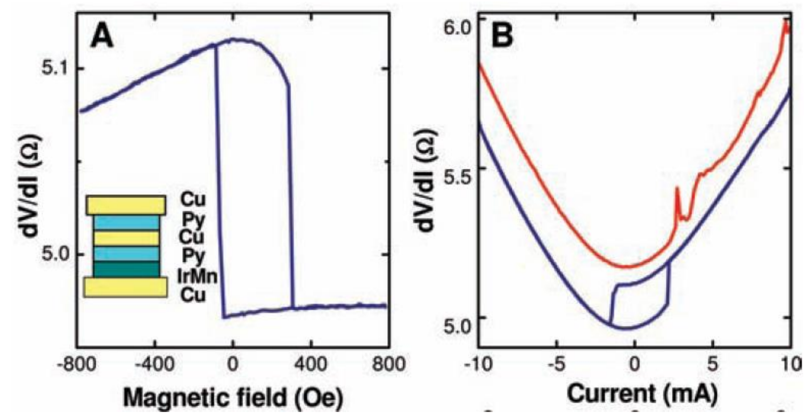

point contact

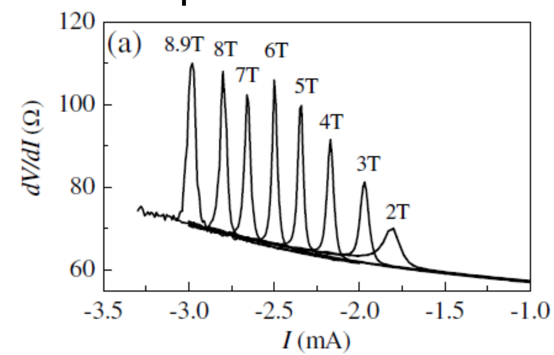

Science **307**, 228 (2005)
PRL **97**, 107204 (2006)

Measurement and simulation results

Reversible domain wall motion induced by dc current in NiFe/Cu/NiFe submicron wires

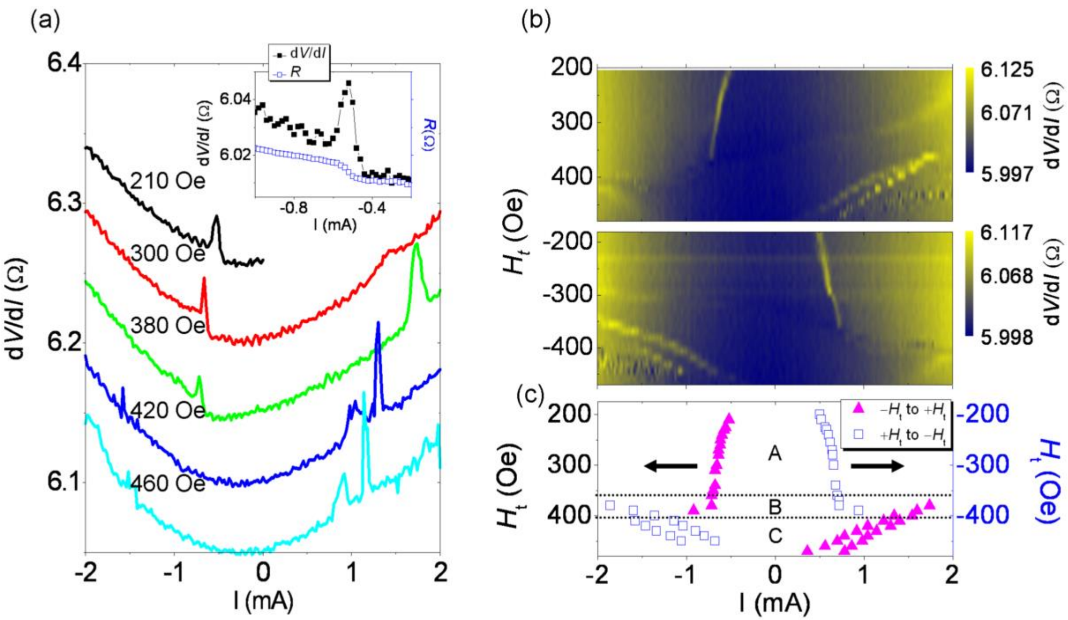

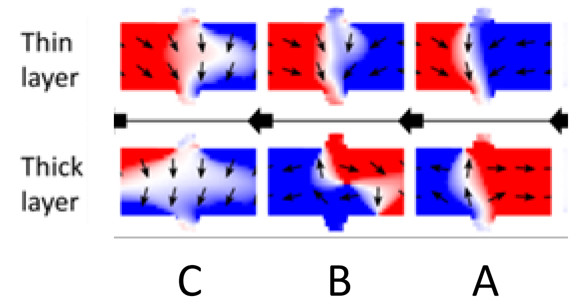

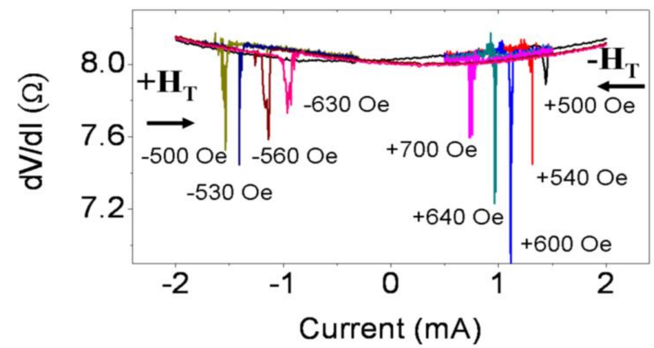

Differential resistance vs. current density at different external transverse fields H_t, enlarged in the inset for V/I vs. j at H_t = 210 Oe. (b) Map of dV/dI versus transverse field and dc current. (c) Critical current I_c vs. H_t.

Measurement and simulation results

Reversible domain wall motion induced by dc current in NiFe/Cu/NiFe submicron wires

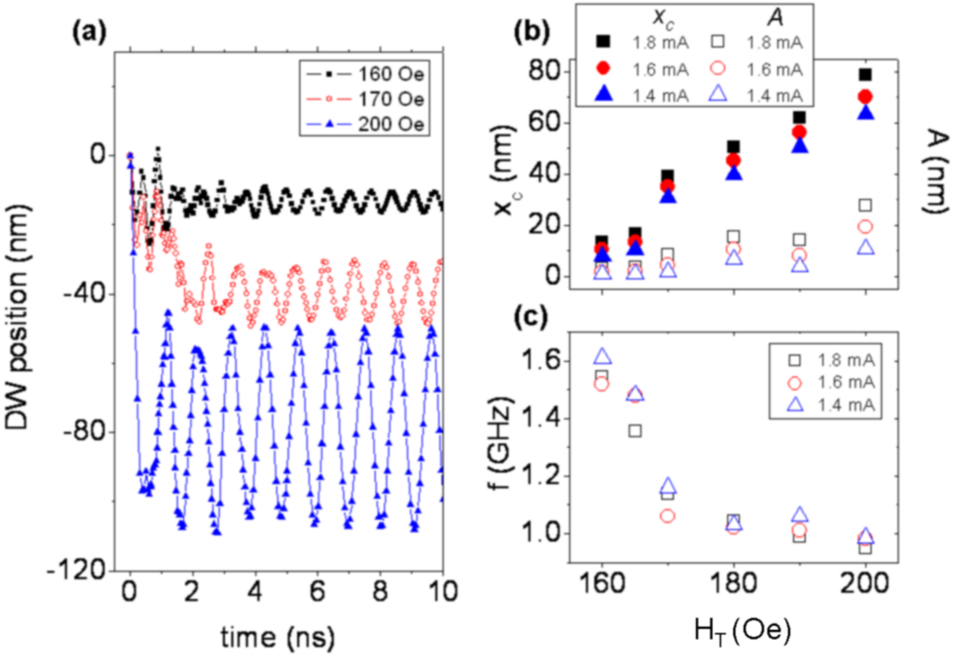

Simulation results of DW position as a function of time under fixed dc current density of 9.7×10^6 A/cm^2 with variation of external transverse field H_t. (b) central position x_c, amplitude A, and (c) frequency of the oscillator vs. H_t with different dc current.

Measurement and simulation results

Reversible domain wall motion induced by dc current in NiFe/Cu/NiFe submicron wires

Series of submicron wires with serial DW traps of artificial symmetric protrusions

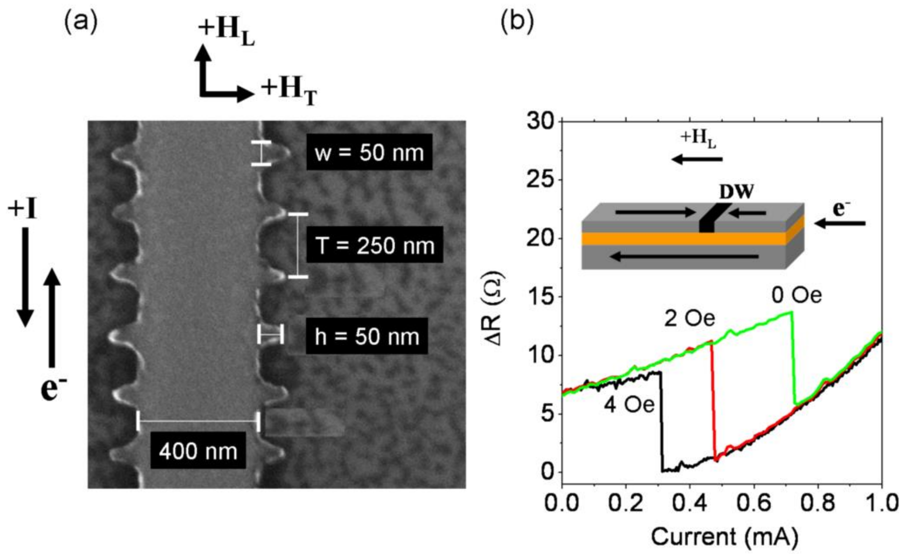

A Scanning electron microscope image of a typical serial-DW-trap sample with the protrusions 50 nm in width and height. The period was 250 nm on either side of the wire. Magnetic field and current directions are specified. (b) Schematic diagram of the sample and the irreversible resistance change from anti-parallel state to parallel state for H_L = 0 (green solid line), 2 (red dash line), and 4 (black dotted line) Oe.

Measurement and simulation results

Reversible domain wall motion induced by dc current in NiFe/Cu/NiFe submicron wires

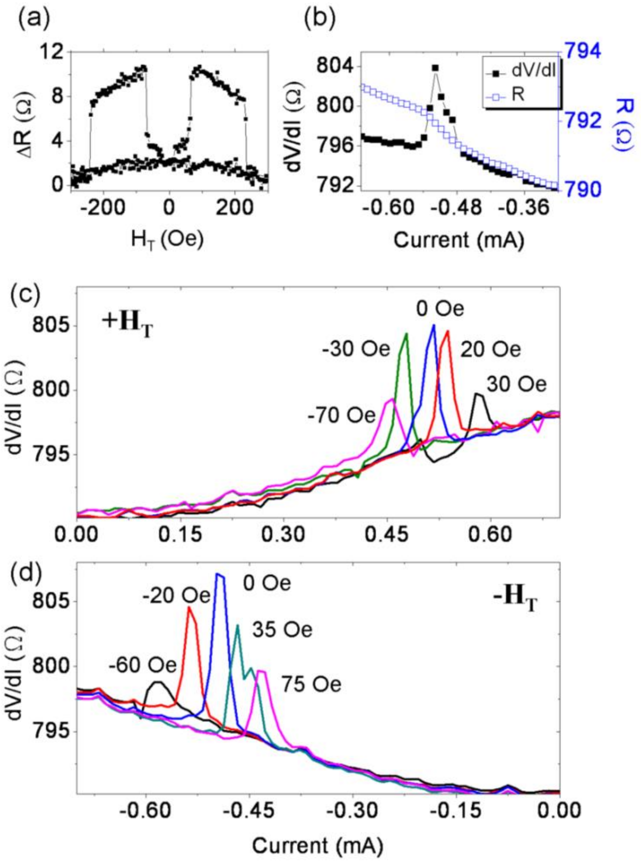

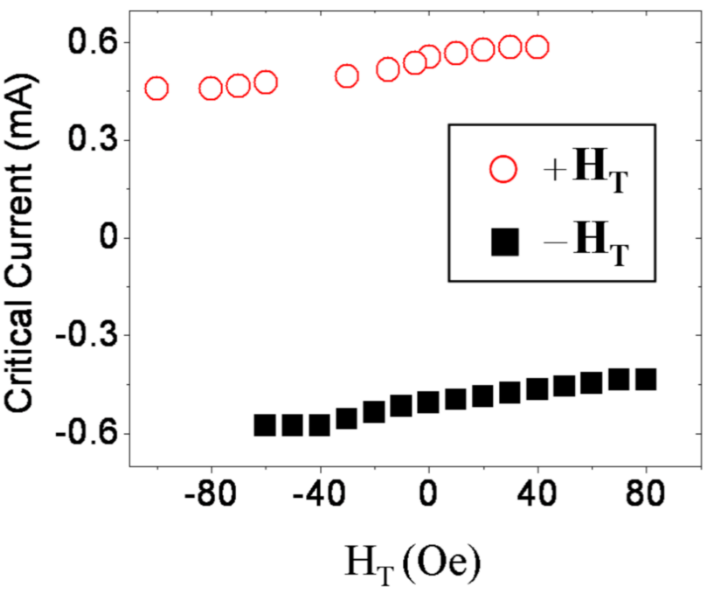

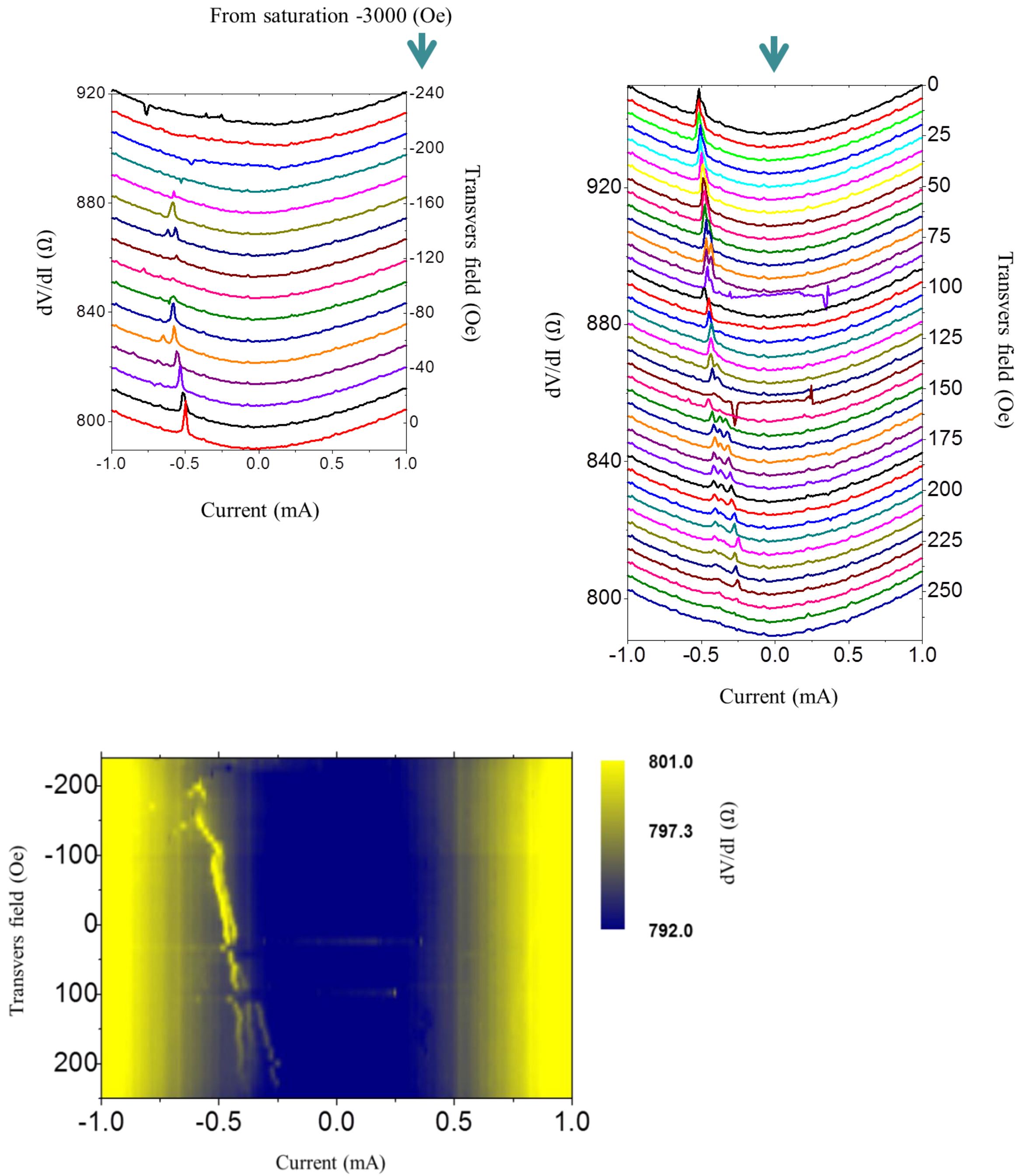
From saturation -3000 (Oe)
dV/dI (Ω)
Transvers field (Oe)
Current (mA)
920
880
840
800
-240
-200
-160
-120
-80
-40
0
-1.0
-0.5
0.0
0.5
1.0
25
50
75
100
125
150
175
200
225
250
-200
-100
100
200
801.0
797.3
792.0

Summary

- DW oscillation with resonance frequency as high as 2.92 GHz and the resonance frequency can be tuned by the width of protrusion.
- The higher resonance frequency for the narrow trap is due to the steeper potential landscape which enhances the restoring force on the pinned DW.
- For the domain wall oscillations induced by injection of a dc current investigated, the observed peak in *dV/dI* associated with the reversible change of magnetoresistance is attributed to the reversible motion of the DW.